

On the Receiver Performance in MU-MIMO Transmission in LTE

Zijian Bai, Stanislaus Iwelski, Guido H. Bruck, Peter Jung Biljana Badic, Tobias Scholand, Rajarajan Balraj
 Department of Communication Technologies Intel Mobile Communications (IMC)
 University of Duisburg-Essen, Oststrasse 99, 47057 Duisburg, Germany Düsseldorf Landstrasse 401, 47259 Duisburg, Germany
 Email: {first.surname}@kommunikationstechnik.org Email: {first.surname}@intel.com

Abstract—Multiuser multiple-input multiple-output (MU-MIMO) transmission scheme has drawn most attentions during the recent development of Long Term Evolution (LTE) systems. Based on the feedback information of the downlink channel, evolved NodeB may achieve multiple accesses via MIMO technology in MU-MIMO Transmission Mode and allow user equipments to share resources in frequency and time domain. In this paper, we review several signal detectors and evaluate their performance in MU-MIMO transmission. The review work aims at the feasibility study of receivers in LTE systems. Different scenarios have been considered in the evaluation progress, e.g. low and high spatial correlation, real channel estimation and feedback delay. Simulation results show that benefits can be obtained by MU-MIMO transmission in the spatial correlated MIMO channel due to the higher condition number in the channel. Besides, reviewed receivers with the co-channel interference-aware signal detection yield good performance compared with single user MIMO receivers. The interference aware receivers are also robust in MU-MIMO transmission with imperfect working conditions, including channel estimation errors and precoding matrix index feedback delay.

Index Terms—LTE (Long Term Evolution), MU-MIMO (Multiuser Multiple Input Multiple Output), Max-Log-MAP (Maximum A Posteriori Probability), IRC (Interference Rejection Combiner)

I. INTRODUCTION

LTE (Long Term Evolution) is the trademarked project name of a high performance air interface for cellular telephone. It is a project of the 3rd Generation Partnership Project (3GPP) for a set of enhancements to the Universal Mobile Telecommunications System (UMTS), hence is termed as E-UTRA (Evolved UMTS Terrestrial Radio Access). The LTE specifications [1] provide downlink peak rates of at least 300 Mbit/s, an uplink of at least 150 Mbit/s associated with 20 MHz channel bandwidth and RAN round-trip time of less than 10 ms. Scalable carrier bandwidths, from 1.4 MHz to 20 MHz, and both frequency division duplexing (FDD) and time division duplexing (TDD) are supported in LTE.

The key technologies in LTE systems are Orthogonal Frequency Division Multiple Access (OFDMA) [2] in the downlink and Single Carrier Frequency Division Multiple Access (SC-FDMA) [3] for uplink transmission. Furthermore, Multi-Input Multi-Output (MIMO) is considered for increasing system capacity in LTE, facilitating spatial multiplexing (SM) and Alamouti based transmit diversity (TxD) schemes.

Besides single user MIMO (SU-MIMO) Transmission Modes, multiuser MIMO (MU-MIMO) transmission is supported as well. MU-MIMO allows base station (eNodeB) to communicate with different radio terminals simultaneously by means of space division multiple access, whereas SU-MIMO only considers access to multiple antennas at a single terminal. The benefit of MU-MIMO transmission is the naturally independent signals cross the antennas mounted at different UEs, which are physically distributed. This allows less restriction on the MIMO channel condition for applying MIMO technology in signal transmission, whereas SU-MIMO requires good uncorrelated signals between antennas at the same user equipment (UE) for SM transmission scheme. MU-MIMO transmission is realized with the precoding and UE pairing in LTE systems, where different precoding matrices or vectors [1] are reported by the paired UEs via feedback channel.

In this paper, we look at different signal receivers and evaluate their performance in MU-MIMO transmission in LTE systems. Related work has been carried out in e.g. [4] and [5] for performance evaluation in system-level. In contrast, we focus on the receiver structures and evaluation of their performance in link-level with realistic working conditions, e.g. channel estimation error, closed-loop feedback delay and different modulation and coding schemes. The aim of the evaluation is to review the reliability and robustness of different receivers in MU-MIMO transmission and to exploit the potential benefits of MU-MIMO transmission in LTE systems compared with SU-MIMO scheme.

In what follows, complex base band notation will be used, deploying matrix vector calculus, for describing the system structure and the signal processing. Discrete-time variables will be denoted by vectors which are given as lower case characters in bold face italics. Matrices will be denoted by upper case characters in bold face italics. Complex values will be underlined. Furthermore, $(\cdot)^H$ denotes the Hermitian of a vector or a matrix, \mathbf{I} is the identity matrix and $E\{\cdot\}$ gives the expectation value of given random variables. $\Re\{\cdot\}$ and $\Im\{\cdot\}$ denote the real and the image parts of the given complex value, respectively.

The reminder of this paper is organized as follows. Section II gives an overview of the LTE system with focus on the precoding matrix index feedback and UE pairing scheme in MU-MIMO transmission. Different MIMO receivers are

discussed in Section III. Section IV summarizes the performance of the receivers in MU-MIMO transmission in different working scenarios in LTE systems. Section V concludes this paper.

II. LTE SYSTEM OVERVIEW

A. System Model

We consider 3GPP 36-series specifications for LTE systems as the baseline for our following discussions. As presented in [6], the system constructed by the LTE physical layer technologies, namely the OFDMA and MIMO, approaches to a bit-interleaved coded modulation (BICM) system [7]. This yields transmissions of the source bits in LTE systems are independent and meet the channel with same quality. The mutual information between transmitted and received bits is maximized in such systems. In what follows, a general system concept of LTE is presented with N_T transmit (Tx) antennas, N_R receive (Rx) antennas and N_L transmission layers (the parallel spatial data streams). Owing to the orthogonality between the subcarriers in each OFDM symbol, we can represent the subcarrier specific SU-MIMO transmission in a single-tap channel scenario in LTE systems by

$$\mathbf{r} = \mathbf{H} \mathbf{P} \mathbf{d} + \mathbf{n}, \quad (1)$$

where $\mathbf{r} \in \mathbb{C}^{N_R}$ represents the received signal vector, $\mathbf{H} \in \mathbb{C}^{N_R \times N_T}$ the MIMO channel matrix, $\mathbf{P} \in \mathbb{C}^{N_T \times N_L}$ the applied precoding matrix, $\mathbf{d} \in \mathbb{C}^{N_L}$ the transmitted signal vector and $\mathbf{n} \in \mathbb{C}^{N_R}$ the additive white Gaussian noise (AWGN) vector at the receiver. Without loss of generality, mutually uncorrelated signal elements are assumed in the transmitted signal vector with covariance matrix $\mathbf{R}_d = E_s \mathbf{I}$ and \mathbf{n} is a zero mean circularly symmetric complex Gaussian (ZMCSCG) random vector with $\mathbf{n} \sim CN(\mathbf{0}, N_0 \mathbf{I})$. We further define the elements in \mathbf{d} are drawn from a quadrature amplitude modulation (QAM) constellation $M = 2^Q$, where Q is the number of bits per symbol.

We consider MU-MIMO transmission with N_{UE} UEs by adding $(N_{UE} - 1)$ UE signals into the downlink transmission. The received signals at the k^{th} UE can be represented by,

$$\mathbf{r}_k = \sum_{n_{UE}=1}^{N_{UE}} \mathbf{H}_k \mathbf{P}_{n_{UE}} \mathbf{d}_{n_{UE}} + \mathbf{n}_k, \quad (2)$$

with mutually independent data from different UEs.

Different transmission modes are supported in LTE systems. Transmission Mode 2 and 3 are used for open-loop transmissions with Tx-D and SM [6] [8], respectively. Transmission Mode 4, 5 and 6 are related to the closed-loop transmission with precoding matrix index (PMI) feedback for SU-MIMO SM, MU-MIMO and SU-MIMO with single layer, respectively. In the context of this paper, we concentrate our discussion on Transmission Mode 5 and for the reference purpose Transmission Mode 6.

For Transmission Mode 6 in LTE systems, we represent the system function by setting in $N_L = 1$ (1)

$$\mathbf{r} = \mathbf{H} \mathbf{p} \mathbf{d} + \mathbf{n}, \quad (3)$$

in which the precoding matrix is degraded to be a precoding vector $\mathbf{p} \in \mathbb{C}^{N_T \times 1}$.

For Transmission Mode 5, MU-MIMO transmission, two UEs with single layer to each UE are scheduled in LTE systems [8]. Using (2) and setting $N_{UE} = 2$, we can represent the system function for the k^{th} UE by

$$\mathbf{r}_k = \mathbf{H}_k \mathbf{p}_1 \mathbf{d}_1 + \mathbf{H}_k \mathbf{p}_2 \mathbf{d}_2 + \mathbf{n}_k, \quad k = 1, 2. \quad (4)$$

B. Spatial Channel Model

For benchmarking, 3GPP introduced spatial channel model (SCM) in [9]. In particular, Section A1 and A2 of [9] provide guidelines for the SCM simulations by setting out from the general concept of [10]. In [9] four representative SCM test cases including antenna configurations and realistic antenna correlation properties are introduced, also explicitly considering antenna polarization. The SCM test case SCM-A refers to the suburban macro propagation, SCM-B and SCM-C consider the urban macro cellular environment with either low or wide angle spreads, and SCM-D reflects the case of an urban micro cellular scenario. In the context of this paper, we consider the SCM-B and SCM-D test cases as the baseline to evaluate the system performance of MU-MIMO transmission.

C. PMI Selection

As specified in [6] [8], the closed-loop principle has been introduced in LTE systems downlink transmission by reporting back different information from UE to the eNodeB through the uplink channel in a periodic or aperiodic fashion [8]. The feedback information, the PMI, provides information about the preferred precoding matrix in a codebook based precoding [6]. The reported PMIs from UE help the eNodeB inquiring the knowledge of the downlink channel state information (CSI). Using the channel information a UE severed by eNodeB may find the most suitable precoding matrix which aligns own signals to the own downlink channel state. This procedure helps UEs in both Transmission Mode 5 and Transmission Mode 6 to improve the desired received signal energy. Considering a single transmission layer per UE in those two modes, we conclude that a matched filter (MF) based receiver with maximum likelihood (ML) decision rule will maximize the signal strength for the target UE without prerequisite of the knowledge of Transmission Mode [11]. The MF receiver can be represented by the filter vector

$$\mathbf{m}_k^H = \left(\mathbf{H}_k \mathbf{p}_k \right)^H, \quad k = 1, 2. \quad (5)$$

The corresponding post processing signal to noise ratio (Post-SNR) is given by

$$\gamma_{\text{MF}} = \left\| \mathbf{H}_k \mathbf{p}_k \right\|^2 \gamma, \quad k = 1, 2, \quad (6)$$

with γ being the SNR at each receiver antenna. The most suitable PMI will be selected to maximize the Post-SNR at the output of the MF receiver. Therefore, we may represent the

selection of the best precoding vector \underline{p} by using the following maximum Post-SNR criterion

$$\underline{p}_k = \arg \max_{\underline{p}_i \in \mathcal{P}} \left\| \underline{H}_k \underline{p}_i \right\|^2, \quad k = 1, 2, \quad (7)$$

with \mathcal{P} being the corresponding codebook for particular number of Tx antennas [6].

The above discussion gives the precoding matrix selection in a particular subcarrier. However, the more interesting scenario of PMI selection in LTE systems is the wideband selection due to the limitation of the uplink channel capacity for feedbacks. The wideband PMI selection requires one preferred precoding matrix being selected for a group of subcarriers in LTE systems [8]. The extension of (7) for the wideband precoding matrix selection in a bandwidth of B_{PMI} including N_{subc} subcarriers is

$$\begin{aligned} \underline{p}_k &= \arg \max_{\underline{p}_i \in \mathcal{P}} \sum_{j=1}^{N_{\text{subc}}} \left\| \underline{H}_{k,j} \underline{p}_i \right\|^2 \\ &= \arg \max_{\underline{p}_i \in \mathcal{P}} \left(\underline{p}_i^H \underline{R}_{\text{Tx}} \underline{p}_i \right), \\ k &= 1, 2. \end{aligned}$$

with $\underline{H}_{k,j}$ being the subcarrier specific MIMO channel matrix in the j^{th} subcarrier at the k^{th} UE and $\underline{R}_{\text{Tx}}$ being the estimated transmitter antenna correlation matrix based on the channel matrices in N_{subc} subcarriers [12].

D. UE Pairing in MU-MIMO

A good UE pairing scheme is required at the eNodeB to choose the correct pair of UEs for MU-MIMO transmission in LTE systems. This pairing scheme shall maintain less interference between scheduled UEs in MU-MIMO transmission. A proper pairing scheme can be designed by maximizing the Chordal distance between the feedback precoding matrices of the UEs. The Chordal distance between two matrices is given in [13] and represented by

$$d_{\text{chord}}(\underline{p}_i, \underline{p}_j) = \frac{1}{\sqrt{2}} \left\| \underline{p}_i \underline{p}_i^H - \underline{p}_j \underline{p}_j^H \right\|_{\text{F}} \quad (8)$$

with $\|\cdot\|_{\text{F}}$ being the Frobenius norm of the matrix.

The Chordal distance generalizes the distance between points on the unit sphere through an isometric embedding from complex Grassmann manifold $\mathcal{G}(N_T, N_L)$ to the unit sphere [13]. Assuming an infinite number of UEs served by the current eNodeB, the k^{th} UE with reported precoding matrix \underline{p}_k will be paired with the m^{th} UE, where the m^{th} UE reports precoding matrix \underline{p}_m and the Chordal distance between \underline{p}_k and \underline{p}_m is maximized. With the maximized Chordal distance criterion \underline{p}_m stays in the antipolar position of \underline{p}_k and hence $\left\| \underline{H}_k \underline{p}_m \right\|^2$ is minimized yielding the minimized inter-UE interference in (4).

In summary, the UE pairing scheme for MU-MIMO transmission in LTE systems can be designed in the way of finding

the m^{th} UE for the k^{th} UE based on the reported precoding matrices and the following criterion,

$$\underline{p}_m = \arg \max_{\underline{p}_i \in \mathcal{P}_{\text{UE}}} d_{\text{chord}}(\underline{p}_i, \underline{p}_k). \quad (9)$$

with \mathcal{P}_{UE} being the pool containing all reported precoding matrices at a certain eNodeB.

III. RECEIVER DESIGN FOR MU-MIMO

Typical receivers in a MIMO-OFDM system for spatial multiplexing transmission can be categorized with their signal processing styles, e.g. non-linear and linear receivers [14]. We extend the structure of those receivers for MU-MIMO transmission in this section. Considering the symmetric system function faced by both UEs in MU-MIMO transmission, we simplify our discussion on the receiver structure for the first UE, i.e. $k = 1$ in (4). With the definitions of the effective channel matrix

$$\underline{g}_e = \underline{H}_1 \underline{p}_1, \quad (10)$$

and the interference channel matrix

$$\underline{g}_t = \underline{H}_1 \underline{p}_2, \quad (11)$$

we represent (4) by

$$\underline{r}_1 = \underline{g}_e \underline{d}_1 + \underline{g}_t \underline{d}_2 + \underline{n}_1. \quad (12)$$

A. Linear Block Receiver

The linear block receiver with zero-forcing (ZF) or minimum mean squared error (MMSE) criterion applies linear filter on the received signal vector \underline{r}_1 to compensate the channel distortion and the inter-symbol interference. The output signal vector is the product of the linear filter matrix and the received signals

$$\tilde{\underline{d}}_1 = \underline{m}^H \underline{r}_1. \quad (13)$$

The filter \underline{m} is constructed as

$$\underline{m}_{\text{ZF}}^H = \left(\underline{g}_e^H \underline{g}_e \right)^{-1} \underline{g}_e^H, \quad (14)$$

with ZF criterion and

$$\underline{m}_{\text{MMSE}}^H = \left(\underline{g}_e^H \underline{g}_e + \frac{1}{\gamma} \right)^{-1} \underline{g}_e^H, \quad (15)$$

with MMSE criterion. Due to the single transmission layer per UE in MU-MIMO transmission, we conclude that a linear block receiver with either ZF or MMSE criterion yields the same system performance as the MF filter in MU-MIMO transmission. In (6) the Post-SNR at the output of linear block receivers is calculated. Using the linear block receiver, the UE assumes that interference coming from the paired UE via \underline{g}_t are fully suppressed. However with low resolution or size limited codebooks in LTE, the residual interference is still significant strong and causes an error floor of the signal detection at the first UE. Non-perfect working condition such as feedback delay and channel estimation error will cause more performance degradation.

B. Interference Rejection Combiner

Taking the remaining interference in the received signal vector into account, the receiver can be built in a fashion of suppressing interference and improving the Post-SNR. The interference aware receiver, such as the interference rejection combiner (IRC) in [15] is designed in this manner. We represent the IRC receiver structure in LTE systems here. Following [15], the general IRC structure for the received signal is

$$\underline{\mathbf{m}}_{\text{IRC}}^{\text{H}} = \frac{\underline{\mathbf{g}}_{\text{e}}^{\text{H}} \underline{\mathbf{R}}_{\eta}^{-1}}{\underline{\mathbf{g}}_{\text{e}}^{\text{H}} \underline{\mathbf{R}}_{\eta}^{-1} \underline{\mathbf{g}}_{\text{e}}}, \quad (16)$$

with $\underline{\mathbf{R}}_{\eta}$ being the covariance matrix of the sum of the interference and noise terms,

$$\underline{\mathbf{R}}_{\eta} = \text{E} \left\{ (\underline{\boldsymbol{\eta}} - \text{E} \{ \underline{\boldsymbol{\eta}} \}) (\underline{\boldsymbol{\eta}} - \text{E} \{ \underline{\boldsymbol{\eta}} \})^{\text{H}} \right\}, \quad (17)$$

and

$$\underline{\boldsymbol{\eta}} = \underline{\mathbf{g}}_{\text{t}} \underline{d}_2 + \underline{\mathbf{n}}_1. \quad (18)$$

The IRC introduces a whitening filter $\underline{\mathbf{R}}_{\eta}^{\frac{1}{2}}$ before the modified MF $\underline{\mathbf{g}}_{\text{e}}^{\text{H}} \underline{\mathbf{R}}_{\eta}^{\frac{1}{2}}$ to whiten the interference plus noise with respect to sending signals. Hence the IRC receiver performs linear operations and improves the Post-SNR by suppressing interference and noise terms at the same time. The Post-SNR at the output of the IRC receiver can be represented by

$$\gamma_{\text{IRC}} = \underline{\mathbf{g}}_{\text{e}}^{\text{H}} \underline{\mathbf{R}}_{\eta}^{-1} \underline{\mathbf{g}}_{\text{e}}. \quad (19)$$

C. Max-Log-MAP Receiver

A Max-Log-MAP (Max-Log maximum a posteriori) receiver is presented in [7] for calculating the bit metric of bits in transmitted signals based on the BICM concept and the Max-Log-MAP criterion. An extension of the bit metric calculation on LTE MU-MIMO transmission in (4) may be represented by

$$\Lambda^i(\mathbf{r}_1, c_i = b) = \min_{\underline{d}_1 \in \chi_{1,c_i}^b, \underline{d}_2 \in \chi_2} \left\| \mathbf{r}_1 - \underline{\mathbf{g}}_{\text{e}} \underline{d}_1 - \underline{\mathbf{g}}_{\text{t}} \underline{d}_2 \right\|^2, \quad (20)$$

$$i = 1, 2, \dots, Q,$$

with χ_{1,c_i}^b being the subset of the signal set χ_1 for \underline{d}_1 in constellation with $b \in \{0, 1\}$ in bit position i and χ_2 being the signal set for \underline{d}_2 . Based on bit metric values for a particular bit in symbols, the soft decision output or the log-likelihood ratio (LLR) of the bit is given as

$$\Lambda_{\text{LLR}}^i(\mathbf{r}_1, c_i) = \Lambda^i(\mathbf{r}_1, c_i = 1) - \Lambda^i(\mathbf{r}_1, c_i = 0). \quad (21)$$

Different to the linear operations given in linear receivers, the Max-Log-MAP receiver applies non-linear operations on the received signal vector and requires more computation effort when the constellation size increases. Besides, (20) requires full-bloom search in two different constellations, namely χ_1 and χ_2 for desired signals and interference signals, respectively.

Table I
SIMULATION PARAMETERS

Parameter	Value
System Bandwidth	10 MHz
Data Subcarriers	600
FFT Size	1024
Cyclic Prefix Length	80 × 1, 72 × 6 in one slot
Subframe/Slot Length	14 OFDM / 7 OFDM in one slot
Channel Model	SCM-B, SCM-D [9]
MIMO	4 × 2 for $N_{\text{T}} \times N_{\text{R}}$
UE Velocity	3 km/h, 30 km/h
Channel Estimation	Ideal Channel Knowledge (ICK), Estimation with cascade one dimensional Wiener interpolator (1DW) [17]
Receiver	MF filter, IRC, Max-Log-MAP [16]
Transmission Modes	MU-MIMO and SU-MIMO
Channel Coding	Turbo codes
Modulation and coding scheme	CQI=4, 7, 10, 13 in [8]
PMI Selection	One PMI for system bandwidth with MaxSNR criterion in Section II-C
UE pairing	Infinite number of UEs available for pairing with criterion in Section II-D
Closed-loop Delay	1 or 8 subframes delay between selection and applying of PMI

IV. SIMULATIONS

In this section, we present the performance of the receivers discussed in Section III. The performance evaluation is carried out by the simulation results obtained from an LTE specification compliant simulator and is presented in terms of coded block error ratio (BLER) versus SNR in all figures, where the SNR refers to the signal to noise ratio per receive antenna. This LTE compliant simulator has been implemented in C/C++ with all physical layer (PHY) processing and different Transmission Modes in [8] as well as a spatial channel model given in Section II-B.

The executed simulations have been configured following the parameters for LTE system PHY [6]. Table I gives the additional parameters used for obtaining the simulation results presented in this section with Table II containing corresponding transport block sizes, modulation orders and the code rates for the selected CQI values. We select the SCM-B and SCM-D test cases as the simulation scenarios to carry out the MU-MIMO transmission performance in high and low spatial correlated channels, respectively. To obtain the coded system performance with linear receivers, the soft bits after linear operations are generated by following the LLR value computation method in [16].

The performance of the different receivers under the SCM-D 4 × 2 channel model with the UE velocity of 3 km/h and 30 km/h are depicted in Figure 1 and Figure 2, respectively. Being a reference, system performances in Transmission Mode 6 with the MF receiver are also plotted. In both Figure 1 and Figure 2, the simple MF receiver gives the worst performance for the signal detection in MU-MIMO

Table II
CQI VALUES AND THE CORRESPONDING TRANSPORT BLOCK SIZES

CQI	Modulation	Code Rate	Transport Block Size [8]
4	QPSK	0.301	3624
7	16QAM	0.369	8760
10	64QAM	0.455	16416
13	64QAM	0.754	27376

Transmission Mode. With CQI = 4, i.e. QPSK modulation, the MF receiver provides similar performance as the other receivers. However, for large CQI values, the MF receiver faces error floor. More than 50% blocks cannot be decoded successfully by the MF receiver with CQI = 10 and CQI = 13. The MF receiver is unaware of the co-channel interference given by the interferer UE in MU-MIMO transmission and hence suffers the strong degradation caused by the interference. Such co-channel interference increases when the modulation order increases. Similar to the MF receiver, the IRC receiver deploys linear operation as well and has quite similar performance as the Max-Log-MAP receiver. The maximum performance difference between the IRC and Max-Log-MAP receivers is about 1 dB and 2 dB at $\text{BLER} = 10^{-2}$ in 3 km/h and 30 km/h scenarios, respectively. Compared with the lower UE velocity, the higher UE velocity shifts the receiver performance by 2 dB for both IRC and Max-Log-MAP receivers. This is caused by the mismatching between the reported optimal PMI and the real channel matrices when the precoding matrices are applied. The higher the UE velocity is, the stronger is the mismatching, and therefore the worse is the receiver performance. However, this impact is limited by 2 dB from 3 km/h to 30 km/h which is acceptable for real systems. Comparing the performance between the Transmission Mode 5 and Transmission Mode 6, we conclude that the co-channel interference causes significant performance loss in Transmission Mode 5. The increased modulation order (e.g. CQI = 10 or 13) generates stronger interference and therefore causes more performance loss in Transmission Mode 5. However, this loss can be compensated by serving more UEs in Transmission Mode 5 than in Transmission Mode 6, yielding a higher system throughput.

Figure 3 presents the performance of different receivers under the SCM-B 4×2 scenario with the same system settings as in Figure 1. The MF receiver still suffers large performance degradation or error floor issue in SCM-B channel. Due to the higher spatial correlation in SCM-B than in SCM-D both the IRC and the Max-Log-MAP receivers obtain 1 to 2 dB gain at $\text{BLER} = 10^{-2}$ in SCM-B channel. This can be explained that each UE in MU-MIMO transmission receives the desired signal only through single layer, which may be aligned to the better sub-channel associated with the dominated eigenvalue from the channel matrix. The stronger spatial correlation yields a larger condition number. That means the UE obtains more channel gain for the desired signals and has less interference from the co-channel interferer UE, which leads to higher signal to interference and noise ratio (SINR) per subcarrier. However,

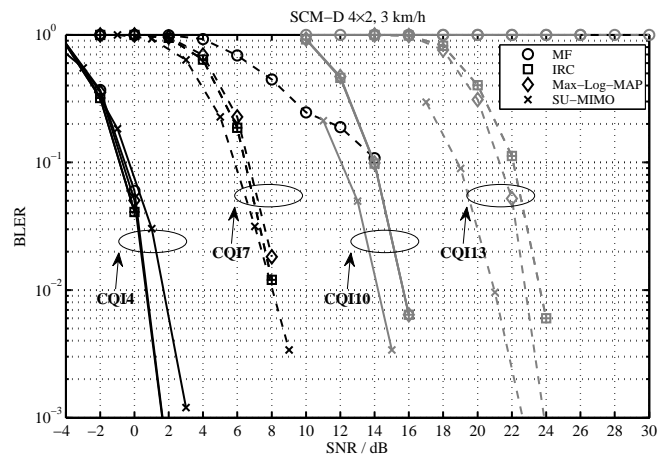


Figure 1. Performance in SCM-D 4×2 with ICK and 3 km/h UE Velocity

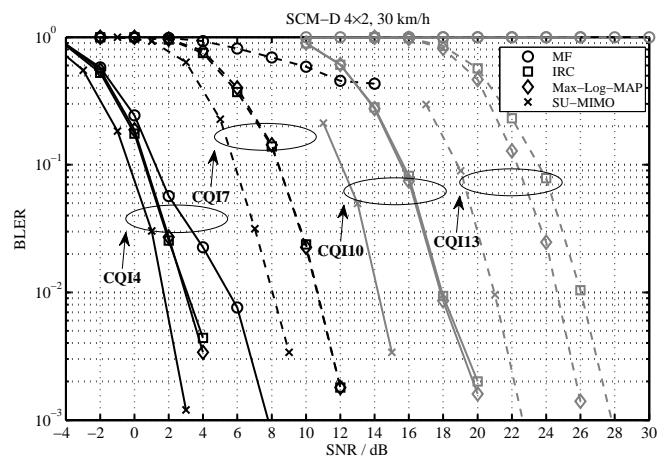


Figure 2. Performance in SCM-D 4×2 with ICK and 30 km/h UE Velocity

this performance gain vanishes with CQI = 13. In this case, there is less coding gain due to the higher modulation order and higher code rate. The potential performance gain given by the improved SINR in higher correlation scenarios cannot compensate the loss given by strong frequency selectivity in SCM-B channel, which has longer power delay profile than SCM-D.

Instead of using ideal channel knowledge, performances of receivers in Figure 4 are presented by using the real channel estimator. Besides that, the delay between the PMI selection and applying the corresponding precoding matrices at the transmitter is set to be 8 subframes instead of 1 subframe. Under these real working conditions both the IRC and the Max-log-MAP receivers have 2 to 3 dB performance degradation compared to the results in Figure 3. This degradation is caused by the channel estimation error and the mismatching between the reported optimal PMI and the real channel matrices when the precoding matrices are applied (similar effects caused by high UE velocity). However, the IRC receiver still has quite similar performance as the Max-Log-MAP receiver under those non-perfect working conditions. Therefore we conclude

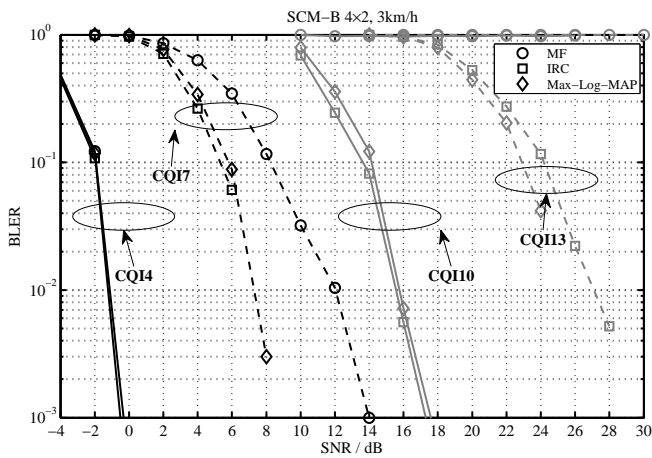


Figure 3. Performance in SCM-B 4x2 with ICK and 3 km/h UE Velocity

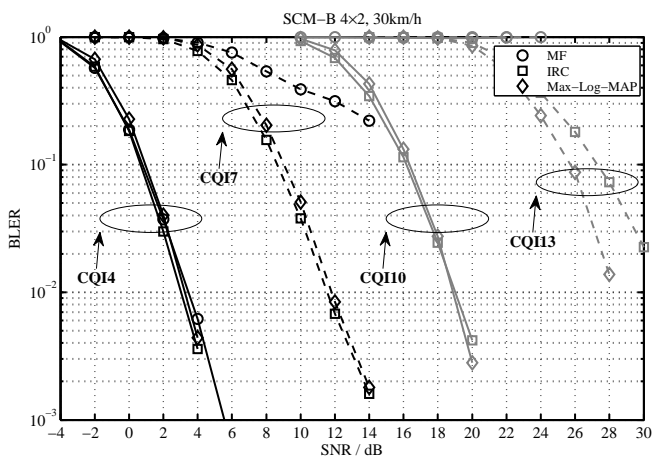


Figure 4. Performance in SCM-B 4x2 with 1DW and Feedback Delay of 8 Subframes

that the IRC receiver is robust for MU-MIMO transmission in LTE systems.

V. CONCLUSION

In this paper, we presented the system performance in MU-MIMO transmission with different receivers in LTE systems. In addition, we presented the Max-SNR based simple PMI selection and the maximum Chordal distance based UE pairing criteria for MU-MIMO transmission. It has been shown that receivers with consideration of the co-channel interference, e.g. the IRC and Max-Log-MAP receivers, provide good performance in MU-MIMO transmission with perfect or non-perfect working conditions (channel estimation error and feedback delay), whereas the simple linear filter receiver faces large performance degradation or error floor issue. It has been demonstrated that a spatial correlated scenario helps the receivers to obtain the performance gain by eliminating the co-channel interference in MU-MIMO transmission.

ACKNOWLEDGMENT

The authors wish to gratefully acknowledge the support of their colleagues at Intel Mobile Communications and at the Department of Communication Technologies of University of Duisburg-Essen. Parts of this work are carried out within the scope of the SAMURAI project which has been partially funded by the European Commission under FP7.

REFERENCES

- [1] 3GPP36.201, "Evolved Universal Terrestrial Radio Access (E-UTRA); LTE physical layer; General description," 3GPP, Sophia Antipolis, Technical Specification 36.201 v8.3.0, Mar. 2009.
- [2] H. Yin and S. Alamouti, "OFDMA: A broadband wireless access technology," in *IEEE Sarnoff Symposium (SARNOFF)*, Mar. 2006, pp. 1-4.
- [3] H. G. Myung, J. Lim, and D. J. Goodman, "Single carrier FDMA for uplink wireless transmission," *IEEE Vehicular Technology Magazine*, vol. 1, no. 3, pp. 30-38, Sep. 2006.
- [4] C. Ribeiro, K. Hugl, M. Lampinen, and M. Kuehler, "Performance of linear multi-user MIMO precoding in LTE system," in *Proceedings of the 3rd International Symposium on Wireless Pervasive Computing (ISWPC 2008)*, Santorini, May 2008, pp. 410-414.
- [5] P. Frank, A. Müller, and J. Speidel, "Fair Performance Comparison between CQI- and CSI-based MU-MIMO for the LTE Downlink," in *Proceedings of European Wireless Conference*, Lucca, Apr. 2010.
- [6] 3GPP36.211, "Evolved Universal Terrestrial Radio Access (E-UTRA); Physical Channels and Modulation," 3GPP, Sophia Antipolis, Technical Specification 36.211 v8.9.0, Dec. 2009.
- [7] G. Caire, G. Taricco, and E. Biglieri, "Bit-interleaved coded modulation," *IEEE Transactions on Information Theory*, vol. 44, no. 3, pp. 927-946, May 1998.
- [8] 3GPP36.213, "Evolved Universal Terrestrial Radio Access (E-UTRA); Physical layer procedures," 3GPP, Sophia Antipolis, Technical Specification 36.213 v8.8.0, Sep. 2009.
- [9] 3GPP25.814, "Physical layer aspect for evolved Universal Terrestrial Radio Access (UTRA)," 3GPP, Sophia Antipolis, Technical Report 35.814 v7.1.0, Sep. 2006.
- [10] 3GPP25.996, "Spacial channel model for Multiple Input Multiple Output (MIMO) simulations," 3GPP, Sophia Antipolis, Technical Report 25.996 v8.0.0, Dec. 2008.
- [11] J. R. Barry, E. A. Lee, and D. G. Messerschmitt, *Digital Communication*, 3rd ed. New York: Springer, Sep. 2003.
- [12] M. Herdin, N. Czink, H. Ozelik, and E. Bonek, "Correlation matrix distance, a meaningful measure for evaluation of non-stationary MIMO channels," in *Proceedings of IEEE 61st Vehicular Technology Conference (VTC 2005-Spring)*, Stockholm, May-Jun. 2005, pp. 136-140.
- [13] D. Love and R. Heath, "Limited feedback unitary precoding for spatial multiplexing systems," *IEEE Transactions on Information Theory*, vol. 51, no. 8, pp. 2967-2976, Aug. 2005.
- [14] Z. Bai, J. Berkmann, C. Spiegel, T. Scholand, G. Bruck, C. Drewes, B. Gunzelmann, and P. Jung, "On MIMO with successive interference cancellation applied to UTRA LTE," in *Proceedings of the 3rd International Symposium on Communications, Control and Signal Processing (ISCCSP 2008)*, Malta, Mar. 2008, pp. 1009-1013.
- [15] M. Escartin and P. Ranta, "Interference rejection with a small antenna array at the mobile scattering environment," in *Proceedings of the first IEEE Signal Processing Workshop on Signal Processing Advances in Wireless Communications (SPAWC)*, Paris, Apr. 1997, pp. 165-168.
- [16] A. Viterbi, "An intuitive justification and a simplified implementation of the map decoder for convolutional codes," *IEEE Journal on Selected Areas in Communications*, vol. 16, no. 2, pp. 260-264, Feb. 1998.
- [17] C. Carbonelli and S. Franz, "Analytic performance evaluation of MIMO OFDM with pilot-aided channel estimation on doubly selective channels," *Telecommunications, European Transactions*, vol. 21, no. 7, pp. 589-602, 2010.